



Nuclear Considerations for FIRE

M.E. Sawan and H.Y. Khater

January 2002

UWFDM-1162

Presented at the 19th IEEE/NPSS Symposium on Fusion Engineering (SOFE), 22–25 January 2002, Atlantic City NJ.

FUSION TECHNOLOGY INSTITUTE

UNIVERSITY OF WISCONSIN

MADISON WISCONSIN

DISCLAIMER

This report was prepared as an account of work sponsored by an agency of the United States Government. Neither the United States Government, nor any agency thereof, nor any of their employees, makes any warranty, express or implied, or assumes any legal liability or responsibility for the accuracy, completeness, or usefulness of any information, apparatus, product, or process disclosed, or represents that its use would not infringe privately owned rights. Reference herein to any specific commercial product, process, or service by trade name, trademark, manufacturer, or otherwise, does not necessarily constitute or imply its endorsement, recommendation, or favoring by the United States Government or any agency thereof. The views and opinions of authors expressed herein do not necessarily state or reflect those of the United States Government or any agency thereof.

Nuclear Considerations for FIRE

M.E. Sawan and H.Y. Khater

Fusion Technology Institute
University of Wisconsin
1500 Engineering Drive
Madison, WI 53706

January 2002

UWFDM-1162

Presented at the 19th IEEE/NPSS Symposium on Fusion Engineering (SOFE), 22–25 January 2002,
Atlantic City NJ.

Abstract—Nuclear analyses have been performed for the baseline design of the Fusion Ignition Research Experiment (FIRE). Nuclear heating, structural radiation damage, and magnet insulator dose were evaluated. Critical issues requiring additional R&D effort include low-temperature embrittlement of copper and identifying insulators that can handle a dose as high as 1.5×10^{10} Rads under the FIRE load conditions. Activation calculations were performed to determine the amount of radioactivity and decay heat generated. Accessibility for hands-on maintenance was assessed. All components qualify as low level waste.

I. INTRODUCTION

FIRE is a compact high field tokamak that utilizes cryogenically cooled copper coils [1]. The design is in the preconceptual design phase where many different design options and operating scenarios are being considered. DT pulses with widths up to 20 s and fusion powers up to 200 MW producing a total of 5 TJ fusion energy are planned. In addition, DD pulses with different widths and fusion powers up to 1 MW yield total fusion energy of 0.5 TJ. The baseline design has a major radius of 2 m and an aspect ratio of 3.8. A cross sectional view of the FIRE baseline design is given in Fig. 1. The dimensions are in mm. The average neutron wall loading during the 200 MW DT pulses is 3 MW/m^2 . FIRE utilizes 16 wedged Cu TF magnets with beryllium copper in the inner legs and OFHC copper in the outer leg. A 316SS coil case is used in the outboard (OB) side. A double walled vacuum vessel (VV) with integral shielding has been adopted. The VV thickness varies poloidally from 5 cm in the inboard (IB) region to 54 cm in the OB region. The VV consists of 1.5 cm thick inner and outer facesheets made of 316SS. The space between the VV facesheets includes 60% 304SS and 40% water. A 1.5 cm thick layer of thermal insulation is attached to the back of the coil-side VV facesheet.

The plasma facing components (PFC) include Be coated Cu first wall (FW) and divertor plates made of tungsten rods mounted on a water-cooled Cu heat sink. Two design options were considered for the FW/tiles with passive cooling and active water-cooling of vessel cladding. The impact of these design options on the nuclear parameters in the different components of FIRE was assessed [2]. The design option with water-cooled vessel cladding was chosen as the baseline design to reduce the VV thermal stresses. In this design, the FW/tiles consist of 0.5 cm Be PFC (90% Be), 1.8 cm Cu tiles (80% CuCrZr) and 0.2 cm gasket (50% Cu). A 2.5 cm water-cooled Cu (80% CuCrZr, 15% water) vessel cladding is employed behind the tiles. Detailed calculations were performed for the outer divertor that is exposed to the most severe conditions in the divertor region. The front layer is a

0.5 cm W brush followed by a 2 cm water-cooled CuCrZr heat sink which is attached mechanically to a 10 cm thick water-cooled 316SS backing plate.

Nuclear analysis was performed for the baseline design to evaluate the expected nuclear performance parameters. The neutronics and shielding calculations were performed using the ONEDANT module of the DANTSYS 3.0 discrete ordinates particle transport code system [3]. The activation analysis was performed using the DKR-PULSAR2.0 activation code system [4]. The most recent FENDL-2 data was used in both neutronics and activation calculations. Both the IB and OB regions were modeled simultaneously to account for the toroidal effects. The machine is assumed to have an operation schedule of four pulses per day with 3 hours between pulses.

II. NUCLEAR HEATING

Nuclear heating deposited in the different components was determined and used in the thermal analysis. The calculations were performed for the DT pulses with 200 MW of DT fusion power to determine the largest nuclear heating generated. For the DD pulses with the largest fusion power (1 MW), nuclear heating values are at least two orders of magnitude lower than the values for the 200 MW DT pulses. Table I gives the peak power density values in the different components at the chamber midplane for the baseline design. Fig. 2 gives the nuclear heating distribution in the OB VV at midplane for the baseline design. Nuclear heating in the VV drops by an order of magnitude in ~ 18 cm. The largest power density values in the magnet occur in the IB region at midplane. Nuclear heating in the IB magnet drops by an order of magnitude in ~ 28 cm. Table II lists the peak nuclear heating values at the outer divertor. Relatively high nuclear heating is deposited in the W PFC.

TABLE I
Peak Nuclear Heating (W/cm^3) at Midplane

	IB	OB
Be PFC	33.3	35.6
Cu Tiles	46.9	46.3
Gasket	40.6	40.6
Cooled Cu VV Cladding	40.2	40.1
H ₂ O FW Coolant	27.6	30.9
SS Inner VV Wall	33.8	30.9
SS VV Filer	32.9	28.5
H ₂ O VV Coolant	14.9	15.5
SS Outer VV Wall	30.3	0.07
Microtherm Insulator	9.8	0.02
SS Inner Coil Case	NA	0.038
Cu Magnet	19.5	0.019
SS Outer Coil Case	NA	2.8×10^{-5}

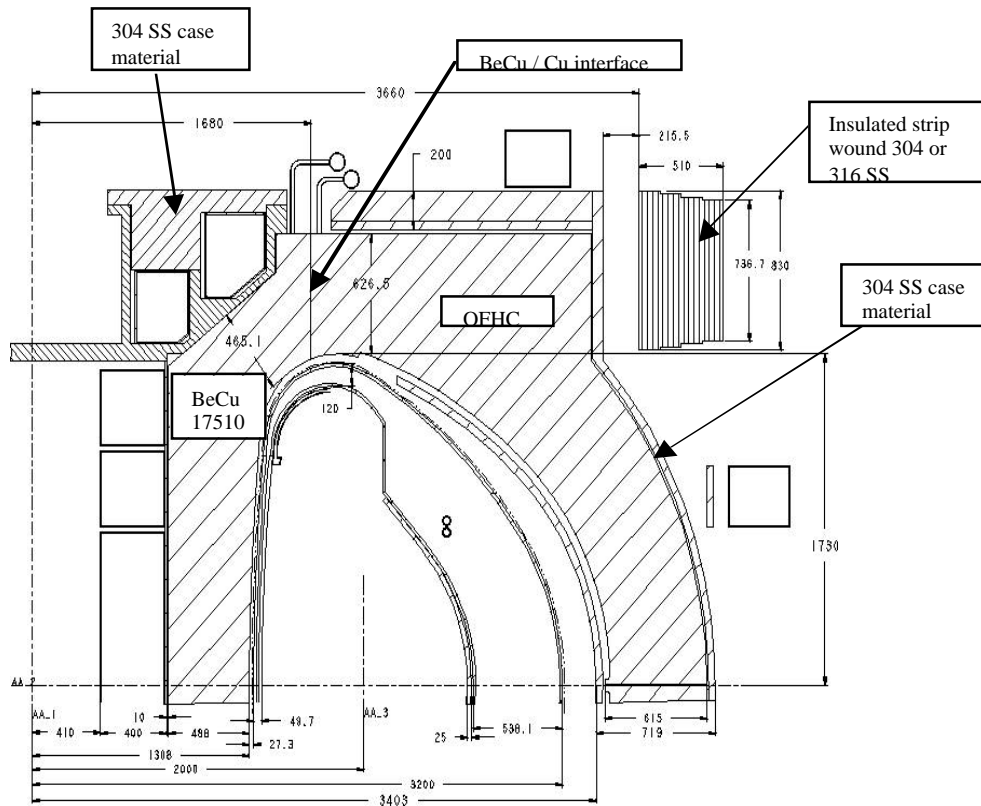


Fig. 1. Cross section of the FIRE baseline design.

TABLE II
Peak Nuclear Heating (W/cm^2) at the Outer Divertor

W rods in divertor	49.0
Cu heat sink in divertor	17.2
SS structure in divertor	14.9
SS VV	6.7
Cu magnet	1.7

neutron wall loading, shielding thickness, and magnet toroidal coverage. Table III gives the breakdown of total magnet nuclear heating for the baseline design. The total heating is dominated by contribution from the lightly shielded IB legs.

TABLE III
Total Magnet Nuclear Heating

	Magnet Nuclear Heating (MW)
IB region	22.9
OB region	0.05
Divertor region	2.1
Total	25.05

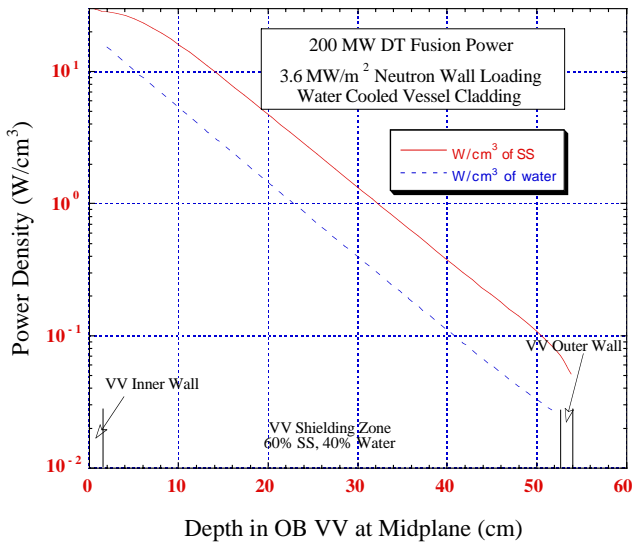


Fig. 2. Nuclear heating distribution in the OB VV.

The total nuclear heating in the 16 TF coils for 200 MW DT fusion power was estimated based on the results of the 1-D calculations taking into account the poloidal variation of

III. RADIATION DAMAGE

The peak cumulative end-of-life radiation damage values were calculated for the FIRE components. For the operation scenario of total DT fusion energy of 5 TJ and total DD fusion energy of 0.5 TJ, the dpa values are very low (< 0.05 dpa). Table IV gives the peak dpa values in the Cu tiles, vessel cladding, Cu finger plates in outer divertor, and Cu TF coils for the FIRE baseline design. Although the damage levels are very low, significant effects on physical and mechanical properties might occur. These effects are strongly dependent on irradiation temperature [5]. Based on the irradiation levels and operation conditions in FIRE and the available data on Cu alloys, data on loss of ductility at temperatures between 80 and 373 K and thermal creep for CuCrZr at high temperatures up to 500°C are needed.

TABLE IV
Peak End-of-life Cu dpa

	Total dpa
IB tiles	0.0327
OB tiles	0.0359
Divertor	0.0150
IB VV cladding	0.0215
OB VV cladding	0.0246
Magnet at IB	0.00666
Magnet at OB	7.54×10^{-6}
Magnet at divertor	4.55×10^{-4}

Since the VV is protected from the fusion neutrons by the thin FW/tiles, the issue of reweldability was addressed. The end-of-life helium production in the VV structure should be limited to 1 appm to allow for rewelding. The peak end-of-life VV He production values in the IB, OB, and divertor regions are 0.11, 0.15, and 0.016 appm, respectively. The contribution from DD shots is very small ($< 0.15\%$). The results imply that reweldability of the VV should not be a concern.

IV. MAGNET INSULATOR DOSE

The insulator dose rate in the TF magnet was calculated at the front layer of the magnet winding pack. For 5 TJ of DT fusion energy and 0.5 TJ of DD fusion energy, Table V provides the peak cumulative magnet insulator dose for the baseline design. The peak value occurs in the lightly shielded IB side at midplane. The dose rate decreases as one moves poloidally to the OB midplane. The relative contribution from DD shots decreases as one moves poloidally from the IB midplane to the OB midplane.

TABLE V
Cumulative Peak Magnet Insulator Dose (Rads)

	Insulator Dose (Rads)	% from DD Shots
IB midplane	1.26×10^{10}	13%
OB midplane	1.26×10^7	1.6%
Divertor	9.80×10^8	10%

The shear strength is the property most sensitive to irradiation. The dose limit used in ITER for epoxies is 10^9 Rads. Polyimides and bismaleimides are more radiation resistant. However, they are difficult to process. Hybrids of polyimides or bismaleimides and epoxies could provide radiation resistant insulators with more friendly processing requirements. The availability, properties, and manufacturing impact of using these insulators is being investigated [6].

In the FIRE design with wedged coils and added compression ring, the TF inner leg insulation does not have to have significant bond shear strength, which is most sensitive to radiation. The peak torsional shear stresses occur at the top and bottom of the IB leg behind the divertor. The end-of-life insulator dose at these locations is reduced to $\sim 10^9$ Rads. The insulator dose decreases as one moves radially from the front to the back of the winding pack as shown in Fig. 3. It is expected that insulation materials will be identified that can

last for the whole device lifetime with the proposed operation scenario and load conditions.

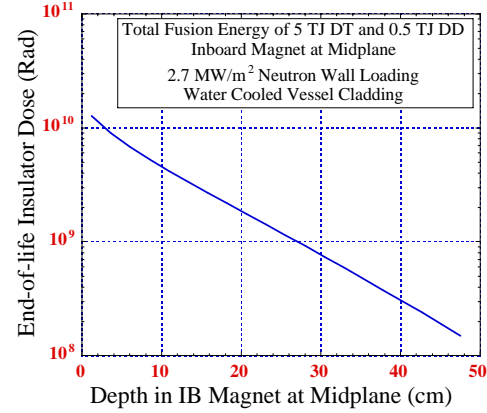


Fig. 3. Radial variation of insulator dose in the IB magnet.

V. ACTIVITY AND DECAY HEAT

Fig. 4 shows the specific decay heat values generated in the OB region for the baseline design. The PFC on the FW and divertor produce the highest levels of specific activity and decay heat. However, the operational schedule with several hours between pulses allows for the decay of short-lived radionuclides between pulses, resulting in low levels of activity and decay heat at shutdown. The activity and decay heat generated following DD shots are at least three orders of magnitude lower than their values following DT shots. The decay heat induced in the FW/tiles, divertor, and Cu magnet at shutdown is dominated by the copper isotopes ^{62}Cu ($T_{1/2} = 9.74$ min) and ^{66}Cu ($T_{1/2} = 5.1$ min). The decay heat induced in the VV at shutdown is dominated by the ^{52}V ($T_{1/2} = 3.76$ min) and ^{56}Mn ($T_{1/2} = 2.578$ hr) isotopes. In general, the short-term activity and decay heat values at shutdown are almost fully dominated by activation during the last pulse.

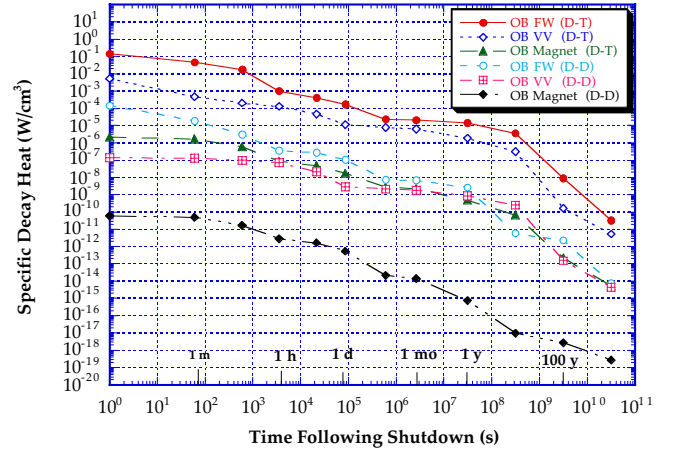


Fig. 4. Decay heat in OB side for baseline design.

VI. BIOLOGICAL DOSE RATES

In order to assess the feasibility of hands-on maintenance, biological dose rates were calculated. Fig. 5 shows the results at midplane as a function of time following DT shots for the baseline design. The biological dose rates behind the VV

remain high for several years following shutdown. The results in Fig. 6 show that following the DD shots, the dose rates behind the VV are five orders of magnitude lower than after DT shots allowing for hands-on maintenance behind the VV. The dose rates behind the magnet at midplane are acceptable for both DD and DT shots. Neutron streaming through the large midplane ports results in excessive dose rates. Our results indicate that using a 110 cm thick steel shield plug in these ports will provide adequate shielding that allows for hands-on maintenance. In addition, the analysis indicated that a 20 cm thick POLY/CAST shield placed above the TF coils results in an acceptable dose at the top of the machine. Both the midplane port plug and the top shield were included in the FIRE baseline design to allow for hands-on ex-vessel maintenance.

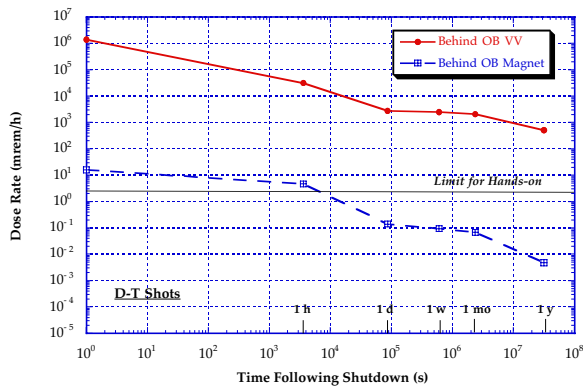


Fig. 5. Biological dose rates at midplane following DT shots.

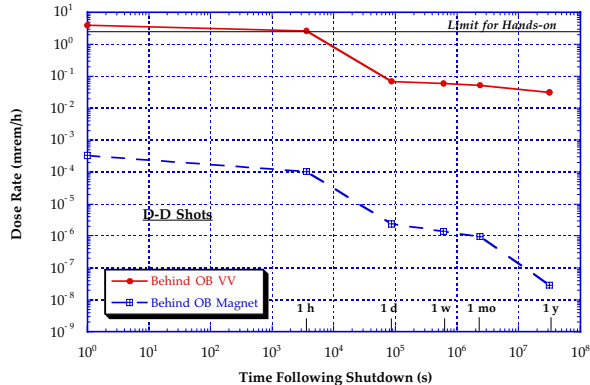


Fig. 6. Biological dose rates at midplane following DD shots.

VII. WASTE DISPOSAL RATINGS (WDR)

The radwaste classification of the different components of the machine was evaluated according to both the NRC 10CFR61 [7] and Fetter [8] waste disposal concentration limits. The results are given in Table VI. The dominant isotopes are given in parentheses. At the end of the machine life, all components would qualify for disposal as Class C low level waste. The IB FW has the largest waste disposal rating. According to Fetter limits, the WDRs are dominated by the silver impurities in the CuCrZr alloy and the niobium impurities in the 316SS and 304SS alloys. The 10CFR61 limits indicate that the WDR values of components made of the CuCrZr alloy are dominated by ^{63}Ni which is produced from copper by the (n,p) reaction. On the other hand, the

WDR values of components made of the steel alloys are dominated by their niobium impurities.

TABLE VI
Class C WDR

Zone	Fetter	10CFR61
IB FW	0.2 ($^{108\text{m}}\text{Ag}$)	0.022 (^{63}Ni)
IB VV	0.092 ($^{108\text{m}}\text{Ag}$, ^{94}Nb)	0.035 (^{94}Nb , ^{63}Ni)
IB Mag.	0.0002 ($^{108\text{m}}\text{Ag}$)	0.0011 (^{63}Ni)
OB FW	0.21 ($^{108\text{m}}\text{Ag}$)	0.024 (^{63}Ni)
OB VV	0.011 ($^{108\text{m}}\text{Ag}$, ^{94}Nb)	0.0032 (^{94}Nb , ^{63}Ni)
OB Mag.	2.26×10^{-6} (^{94}Nb)	2.56×10^{-6} (^{94}Nb , ^{63}Ni)
Divertor	0.034 ($^{108\text{m}}\text{Ag}$)	0.013 (^{94}Nb)

VIII. SUMMARY

Nuclear analyses have been performed for the baseline design of FIRE. Nuclear heating, structural radiation damage, and magnet insulator dose were evaluated. Modest values of nuclear heating occur in the FW, divertor, VV, and magnet. End-of-life He production values imply that the VV will be reweldable. Critical issues for copper alloys used in FIRE requiring additional R&D effort include low-temperature embrittlement and high-temperature thermal creep. Magnet organic insulators with radiation tolerance up to $\sim 1.5 \times 10^{10}$ Rads under FIRE load conditions need to be identified. Activation calculations were performed to determine the amount of radioactivity and decay heat generated. Activity and decay heat values after shutdown are low. Following DT shots hands-on ex-vessel maintenance is possible with the 110 cm shield plug in midplane ports and the 20 cm shield at the top of the TF coils. All components will qualify as Class C low-level waste.

ACKNOWLEDGMENT

Support for this work was provided by the U.S. Department of Energy.

REFERENCES

- [1] D. Meade, "Fusion ignition research experiment (FIRE)," *Fusion Technology*, vol. 39, p. 336, 2001.
- [2] M. Sawan and H. Khater, "Nuclear analysis of the FIRE ignition device," *Fusion Technology*, vol. 39, p. 393, 2001.
- [3] R. Alcouffe et al., "DANTSYS 3.0, One-, two-, and three-dimensional multigroup discrete ordinates transport code system," RSICC Computer Code Collection CCC-547, Contributed by Los Alamos National Lab, August 1995.
- [4] M. Sisolak, Q. Wang, H. Khater and D. Henderson, "DKR-PULSAR2.0: A radioactivity calculation code that includes pulsed/intermittent operation," unpublished.
- [5] S. Fabritsiev, S. Zinkle, and B. Singh, "Evaluation of copper alloys for fusion divertor and first wall components," *Journal of Nuclear Materials*, vol. 233-237, pp. 127-137, 1996.
- [6] M. Tupper et al., "Magnet insulation with resistance to high levels of radiation," *Proceedings of the 16th International Conference on Magnet Technology*, Jacksonville, FL, September 1999.
- [7] Nuclear Regulatory Commission, 10CFR part 61, "Licensing Requirements for Land Disposal of Radioactive Waste," Federal Register, FR 47, 57446, 1982.
- [8] S. Fetter, E. Cheng, and F. Mann, "Long term radioactive waste from fusion reactors," *Fusion Engineering and Design*, vol. 13, pp. 239-246, 1990.